

Soil Microbial Functional Succession Over One Year of Human Decomposition

Allison R. Mason¹, Lois S. Taylor², Naomi Gilbert¹,
Steven W. Wilhelm¹, Jennifer M. DeBruyn^{1,2*}

¹Department of Microbiology, University of Tennessee-Knoxville, 1311
Cumberland Avenue, Knoxville, 37996.

²Department of Biosystems Engineering and Soil Science, University of
Tennessee-Knoxville, 2506 E.J. Chapman Drive, Knoxville, 37996.

*Corresponding author(s). E-mail(s): jdebruyn@utk.edu;

Abstract

During terrestrial vertebrate decomposition, a mix of host- and environmental microbial communities drive biogeochemical cycling of carbon and nutrients. The mixed communities undergo dramatic restructuring in the decomposition hotspots. To reveal the succession of active microbial members and the metabolic pathways they use, we generated metatranscriptomes from soil samples collected over one year from below three decomposing human bodies. Microbes in decomposition soils increased expression of heat shock proteins in response to decomposition products changing physiochemical conditions (*i.e.*, reduced oxygen, high salt). Fungal lipase expression increased implicating fungi as key decomposers of fat tissue. Expression of expression nitrogen cycling genes was phased based on soil oxygen concentrations: during hypoxic soil conditions, genes catalyzing N reducing processes (*e.g.*, hydroxylamine to nitric oxide, nitrous oxide to nitrogen gas during reduce oxygen conditions) were increased, followed by increased expression of nitrification genes once oxygen diffused back into the soil. Increased expression of bile salt hydrolases implicated a microbial

source for the high concentrations of taurine typically observed during vertebrate decomposition. Overall, gene expression profiles remained altered after one year. Together, we show how human decomposition alters soil microbial gene expression, revealing both ephemeral and lasting effects on soil microbial communities.

Keywords: Human Decomposition, Microbial Succession, Metatranscriptomics, Soil Microbial Ecology

Introduction

Soil microbial communities are important drivers of ecosystem processes in terrestrial environments. Many soil microbes are decomposers that are involved in degradation of complex organic matter and drive nutrient cycling in terrestrial ecosystems. Environmental disturbances can impact the presence and/or activity of soil microorganisms that are involved in these cycles, ultimately affecting nutrient availability and the release of greenhouse gas emissions, such as CO₂ and N₂O [1, 2]. Vertebrate death and subsequent carcass deposition in terrestrial ecosystems is one disturbance resulting in the deposition of large quantities of organic C and N [3–10], along with other elements (P, K, S, *etc*) [11], which collectively contribute to microbially-mediated biogeochemical cycling. In addition to this, changes in pH, temperature, and fluctuations in soil oxygen provide abiotic filtering further impacting microbial metabolic strategies [7–9, 11–13]. Decomposition of vertebrate also results in mixing of host and environmental microbes: the animal’s microflora are flushed into the soil along with the decomposition products where they contribute to decomposition processes (*e.g.*, organic nitrogen mineralization) [14].

While C and N transformations have been documented during decomposition, the functional response of microbes and their roles in nutrient cycles remain unclear. The composition and structure of decomposition-impacted soil microbial communities

have been investigated using amplicon sequencing of marker genes (*i.e.*, 16S rRNA, 18S rRNA, ITS). This has allowed us to investigate changes in microbial biodiversity and taxonomic succession in response to vertebrate decomposition, revealing patterns such as increases in the anaerobic taxa *Firmicutes* and *Bacteroidetes* [15]. However, few studies have integrated soil biogeochemistry with microbial community composition, which can further help to describe microbial ecology in human and animal decomposition systems. Taylor et al. (2024) [13] showed that fungal community shifts were linked to changes in soil dissolved oxygen, highlighting interactions between soil microbes and changes in the surrounding environment. While insightful for making potential connections between taxa and environment, these analyses cannot inform which taxa are active members of the community responsible for chemical transformations, which functional pathways/genes are expressed, and how these pathways are altered in response to decomposition.

Methods such as RNA sequencing (*i.e.*, metatranscriptomics) and metabolomics can be used to investigate microbial community functional succession in response to decomposition by measuring gene expression and metabolites, respectively. This can inform how ecological functions, including C and N cycling, are impacted by decomposition events in terrestrial ecosystems. To date, applications of metatranscriptomics to vertebrate decomposition samples have been limited to internal host communities [16, 17]: Burcham et al. (2019) [16] revealed differential expression of amino acid and carbohydrate metabolism in the heart during mouse decomposition, while Ashe et al. (2021) [17] documented taxonomic shifts in gene expression of oral microbial communities during human decomposition.

We expected that soil microbial community, which include a mix of host and environmental taxa, would also have altered gene expression profiles. The decomposition-impacted soil metabolome was assessed by DeBruyn et al. (2021) [18], showing

139 prevalence of amino acids, suggesting upregulation of organic nitrogen metabolic path-
 140 ways. Additionally, DeBruyn et al. (2021) [18] showed the soil metabolome was still
 141 altered compared to starting conditions at the end of the 21-week study, suggesting
 142 long-term impacts of decomposition on soil microbial functioning.
 143
 144 Here, we investigate soil microbial gene expression during a one-year period of human
 145 decomposition. The overarching goal of this work was to assess the impacts of ver-
 146 tebrate decomposition on ecosystem functioning by characterizing community-level
 147 shifts in soil microbial function. We hypothesize that: (i) gene expression would shift
 148 over time as resources are used and transformed and soil chemical and physical condi-
 149 tions change due to the influx of decomposition products during soft tissue degradation
 150 [8, 9, 18]; (ii) expression of genes encoding enzymes involved in nitrogen cycling would
 151 be altered, as changes in nitrogen pools have been previously described in decomposi-
 152 tion soils [8]; (iii) expression of genes involved in lipid metabolism would increase, as we
 153 expect lipids from the body to enter the soil during decomposition and previous studies
 154 identified lipolytic organisms in decomposition soils [12, 19]; (iv) soil expression pro-
 155 files would not return to pre-decomposition conditions after a year, as previous studies
 156 have shown that microbial community composition [20, 21] can remain altered longer
 157 than one year. We analyzed metatranscriptomes of soil samples collected at six key
 158 timepoints over one year of human decomposition to determine the active populations
 159 and expression of genes and pathways relevant to the enhanced biogeochemical cycling
 160 observed in decomposition hotspots. We compared gene expression between decom-
 161 position timepoints and control soils that were unexposed to decomposition products
 162 to identify functions or functional pathways of interest. We show: (i) decomposition
 163 shifts soil microbial community gene expression, and the impacts are still measurable
 164 after one year; (ii) expression of genes related to stress response are elevated in decom-
 165 position soils; (iii) expression of genes encoding triacylglycerol lipase differed between
 166 fungi (increased) and bacteria (decreased); (iv) evidence for phased nitrification and
 167
 168
 169
 170
 171
 172
 173
 174
 175
 176
 177
 178
 179
 180
 181
 182
 183
 184

denitrification, driven by changes in soil dissolved oxygen; (v) evidence for organic sulfur processing (taurine) via bile salt hydrolases. This assessment of functional profiles within decomposition-impacted soils provides insight into the microbial response(s) to vertebrate decomposition in terrestrial settings and biogeochemical cycling within these hotspots.

Results

Soil Physiochemistry

Soil chemistry was altered in response to human decomposition, with multiple parameters still impacted after one year [13]. Generally, soil pH decreased and remained low in decomposition soils of all but one individual. Soil electrical conductivity (EC) increased in response to decomposition, remaining elevated through approximately day 58 before gradually decreasing throughout the remainder of the study (Supplementary Material 1). Respiration (evolved CO₂) increased by an order of magnitude beginning at day 12, which corresponded to a reduction in soil dissolved oxygen (DO) to 29% - 48.9%. Ammonium concentrations increased 78-fold, reaching maximum concentrations between days 12 and 58. This was followed by decreased ammonium and increased nitrate concentrations at day 86, with nitrate concentrations reaching a maximum at day 168 (Supplementary Material 1).

Microbial gene expression in response to human decomposition

Gene expression profiles in decomposition-impacted soils shifted away from controls and day zero samples as decomposition progressed (Fig 1A). Expression was most different from controls on study days 58, 86, 168 (Supplementary Material 2), before shifting back toward control conditions on study day 376. After one year of decomposition, soil gene expression profiles had not returned to pre-decomposition conditions,

231 as evidenced by their clustering away from controls and day zero samples in the MDS
232 plot (Fig 1A).
233

234

235

236

237

238

239

240

241

242

243

244

245

246

247

248

249

250

251

252

253

254

255

256

257

258

259

260

261

262

263

264

265

266

267

268

269

270

271

272

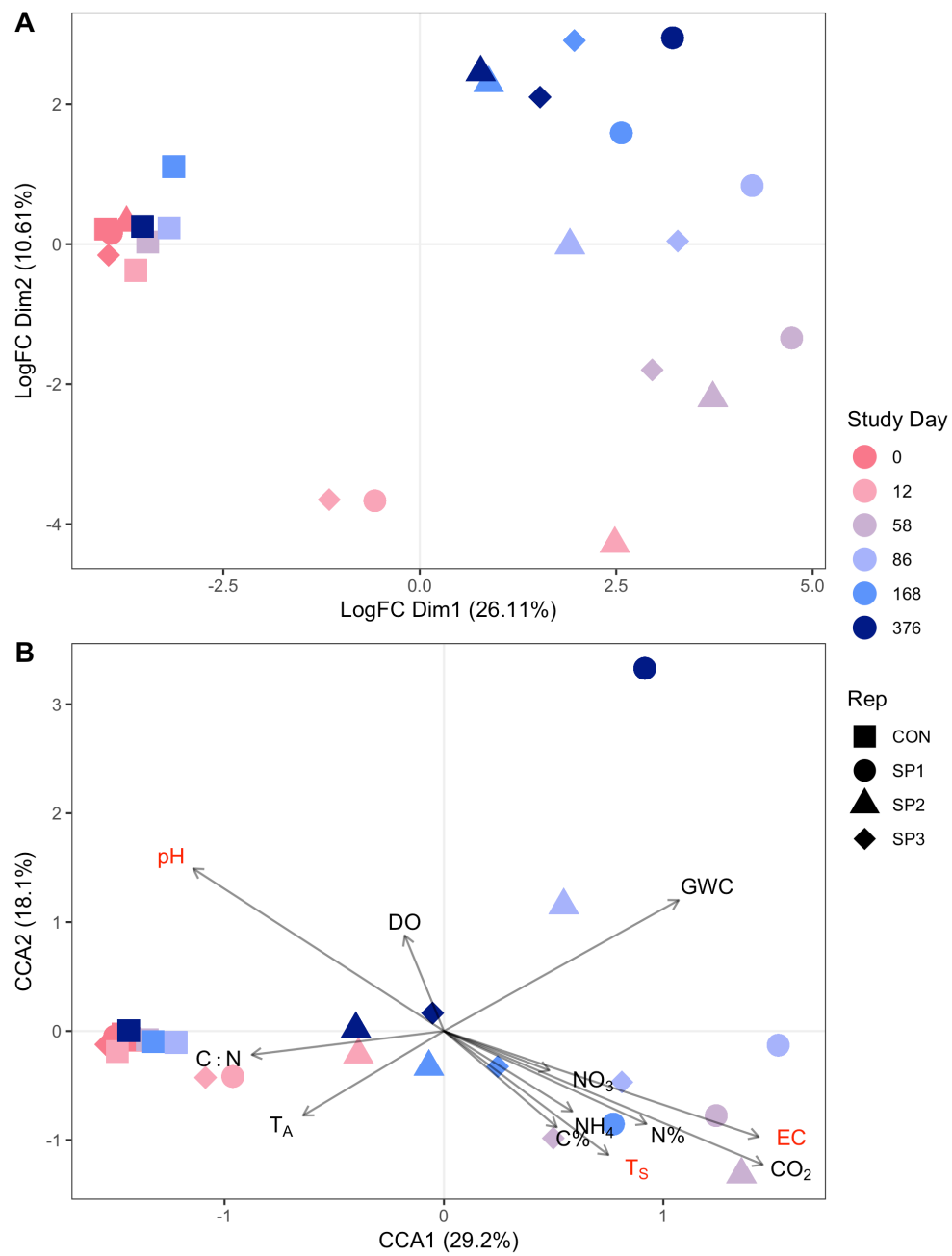
273

274

275

276

Figure 1: Microbial gene expression profiles are altered during human decomposition. Multidimensional scaling (MDS) shows gene expression within soils changed as decomposition progressed (A). Additionally, canonical correspondence analysis (CCA) shows that environmental variables explained 47.3% of the variation in gene expression profiles (B). Variables in bold red type significantly ($p < 0.05$) explained some of the variation in gene expression profiles as assessed by Permutational Analysis of Variance (PERMANOVA). In both panels soils from controls (CON) and the three donors (SP1, SP2, SP3) are denoted by symbol shape, while color represents study day. In B, soil physiochemical variable loadings are represented by arrows: Gravimetric water content (GWC), electrical conductivity (EC), pH (pH), dissolved oxygen (DO), respiration (evolved CO_2 $\mu\text{mol gdw}^{-1}$), ammonium (NH_4), and nitrate (NO_3) concentrations (mg gdw^{-1}), percent carbon (%C), percent nitrogen (%N), carbon:nitrogen ratio (C:N), ambient temperature (T_A), and soil temperature (T_S).



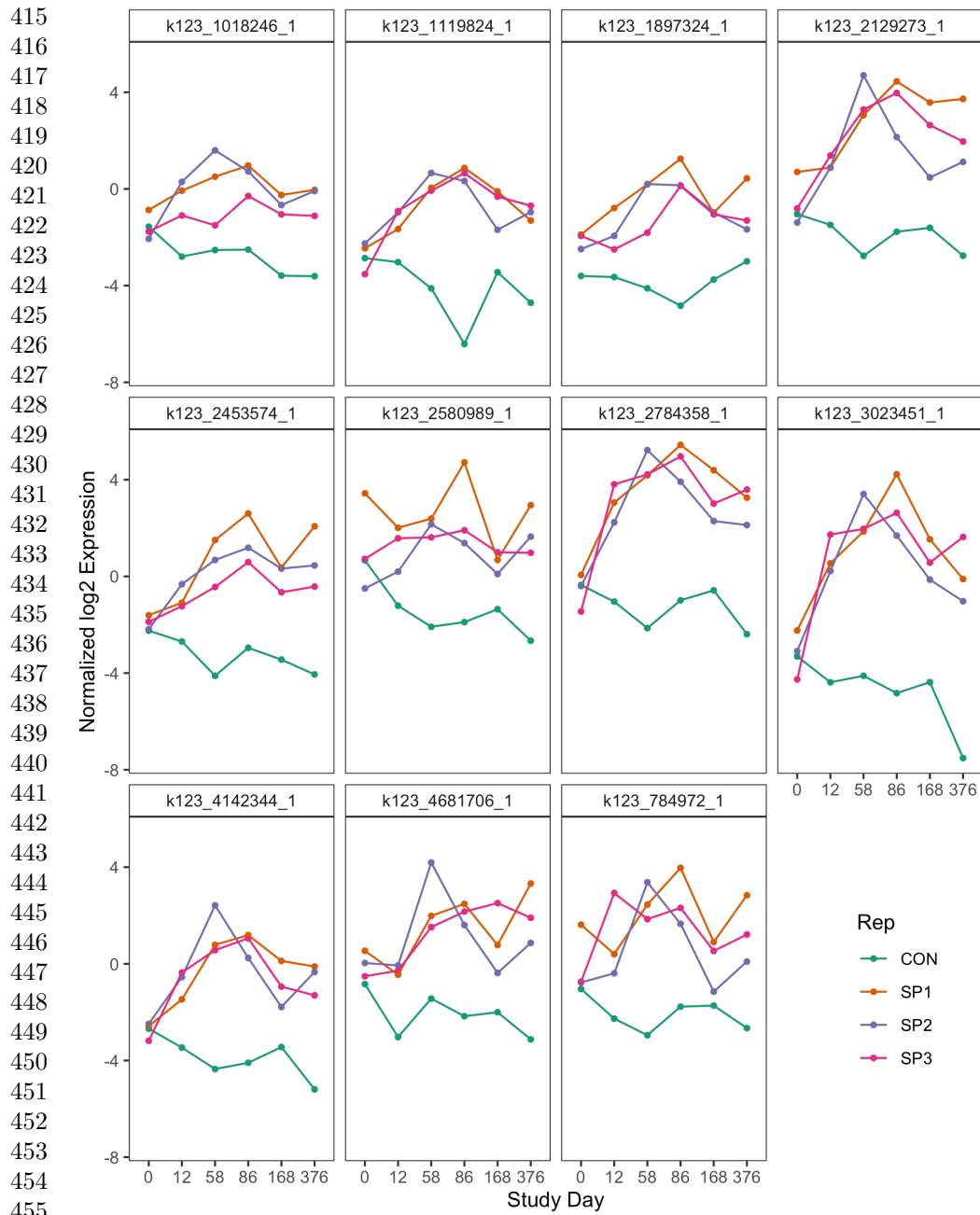
Some correlations were observed between gene expression shifts and soil physiochemical data at decomposition timepoints. Canonical correspondence analysis (CCA) was

323 used to constrain gene expression data with soil physiochemical data (Fig 1B). CCA1
 324 and CCA2 explained 29.2% and 18.1% of the variance in gene expression, respec-
 325 tively. Transcript profiles at day 12 were associated with an increase in soil carbon to
 326 nitrogen ratio (C:N). Gene expression profiles at days 58 to 86 were positively corre-
 327 lated with increased soil temperature, EC, and evolved CO₂, while study day 168 was
 328 associated with elevated levels of soil NO₃. Further, Permutational Analysis of Vari-
 329 ance (PERMANOVA) revealed that internal accumulated degree hours (ADH), soil
 330 temperature, pH, and EC significantly explained some of the variation in gene expres-
 331 sion profiles ($p < 0.05$). No other soil chemical variables were significant at $\alpha = 0.05$
 332 (Supplementary Material 3).

339
 340 Overall, decomposition changed soil gene expression profiles over the one-year study
 341 relative to control soils. Differential expression analysis between decomposition and
 342 control soils identified 7,047 down-regulated and 38,425 up-regulated genes. Gene tran-
 343 scripts that were associated with control soils belonged to a wide variety of clusters of
 344 orthologous genes (COG) functional categories. Specifically, the top 20 genes whose
 345 expression was higher in control soils belonged to ten unique COG categories, includ-
 346 ing signal transduction mechanisms, transcription, and those of unknown function. In
 347 contrast, the top 20 genes whose expression was higher in decomposition soils only
 348 fell into four COG categories (Supplementary Material 4 A): 1) post-translational
 349 modification, protein turnover, and chaperones; 2) energy production and conversion;
 350 3) cell motility; and 4) carbohydrate transport and metabolism. The most common
 351 COG category represented in decomposition soils (80% of the top 20 genes) was post-
 352 translational modification, protein turnover, and chaperones. Within this category,
 353 several heat shock stress response genes were identified, including SSA2, HSP82, and
 354 clpB (Supplementary Material 5). Further investigation into these genes shows their
 355 expression increased in response to decomposition, typically reaching maximum tran-
 356 script levels around study days 58 and 86 (Fig 2). This corresponded to elevated soil
 357
 358
 359
 360
 361
 362
 363
 364
 365
 366
 367
 368

temperatures below decomposing bodies between study days 12-80, with soil temperatures increasing to approximately 43°C [13], and maximum soil EC and minimum dissolved oxygen measurements between days 12 and 58 (Supplementary Material 1).

Figure 2: Normalized log2 expression of heat shock proteins identified by differential expression analysis comparing decomposition and control soils. Each panel represents a single heat shock transcript, labeled with query ID. Symbol color denotes if the sample is a control (CON, green), or one of three individuals: SP1 (orange), SP2 (purple), or SP3 (pink).



415
 416
 417
 418
 419
 420
 421
 422
 423
 424
 425
 426
 427
 428
 429
 430
 431
 432
 433
 434
 435
 436
 437
 438
 439
 440
 441
 442
 443
 444
 445
 446
 447
 448
 449
 450
 451
 452
 453
 454
 455
 456
 457
 458
 459
 460

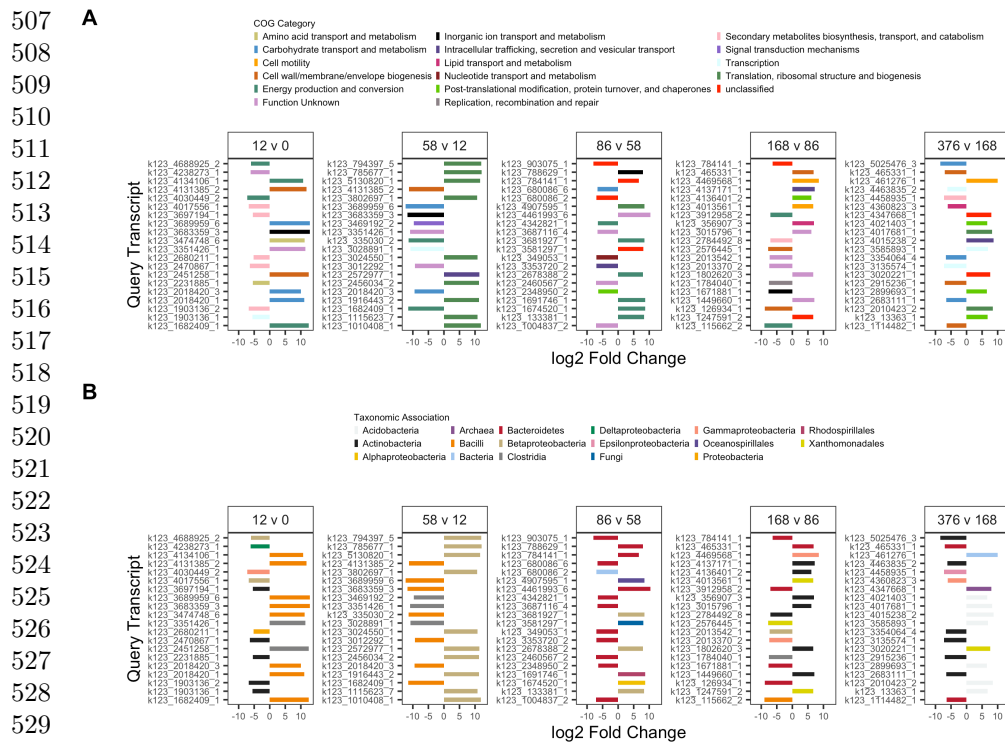
Taxonomy associated with topmost differentially expressed gene transcripts also differed between control and decomposition soils. The top 40 significantly differentially

expressed gene transcripts in decomposition soils were associated with Fungi, *Actinobacteria*, and *Xanthomonadales*, while gene transcripts in controls were associated with *Acidobacteria*, *Cyanobacteria*, *Proteobacteria* (α , δ , γ), and *Planctomycetes* (Supplementary Material 4 B). The greatest number of differentially expressed genes relative to control samples was observed at day 86, where we saw 145,460 and 124,883 up- and down-regulated genes, respectively.

Temporal gene expression show shifts in decomposer functions

Differential expression analysis between respective sequential study days further revealed which genes were altered between decomposition timepoints. The top ten significantly up- and down-regulated genes, determined by the lowest p-values from differential expression analysis (< 0.05), are reported in Supplementary Material 6 and Fig 3.

Figure 3: Top twenty up- and down-regulated genes in decomposition soils comparing sequential study days (0, 12, 58, 86, 168, 376) colored by COG functional category (A) and taxonomic annotation (B). Positive values denote increased expression compared to the preceding timepoint, while negative values denote a decrease.



Expression of genes annotated with the COG categories cell wall/membrane/envelope biogenesis, inorganic ion transport and metabolism, and carbohydrate transport and metabolism increased from day 0 to 12. In contrast, expression of secondary metabolite biosynthesis, transport, and catabolism genes decreased during this period (Fig 3A). Transcripts from *Bacilli* and *Clostridia* increased, while transcripts from *Actinobacteria* decreased between study days zero and 12 (Fig 3).

Between days 12 and 58, 90% of the topmost upregulated genes were associated with the translation, ribosomal structure and biogenesis COG and all were taxonomically associated with *Betaproteobacteria* (Fig 3A,B). Many of these genes were annotated as ribosomal protein large (RPL), involved in ribosomal binding. Genes across multiple COG categories with taxonomic associations to *Bacilli* and *Clostridia* decreased

between study days 12 and 58, six of which were transcripts that previously increased
between days zero and 12 (Fig 3B, Supplementary Material 6).

Multiple transcripts associated with the energy production and conversion COG, as
well as transcripts annotated with the COGs inorganic transport and metabolism,
and translation, ribosomal structure and biogenesis, increased between days 58 and
86 (Fig 3A). Two of the upregulated energy and production and conservation tran-
scripts were associated with cytochrome c oxidase subunits in *Betaproteobacteria*,
while another was annotated as *hao*, encoding the enzyme hydroxylamine dehydroge-
nase which is involved in conversion of hydroxylamine to nitrite during nitrification
(Supplementary Material 6). Further investigation into hydroxylamine dehydrogenase
showed a significant increase in *hao* transcripts at day 86 followed by subsequent
decreases at days 168 and 376 ($F = 4.183$; $p = 0.02$). This increase corresponded to
decreased soil ammonium levels and subsequent accumulation of nitrate (Supplemen-
tary Material 1). Half of the topmost downregulated genes between days 58 and 86
were not assigned to a COG (*i.e.*, unclassified) or were of unknown function.

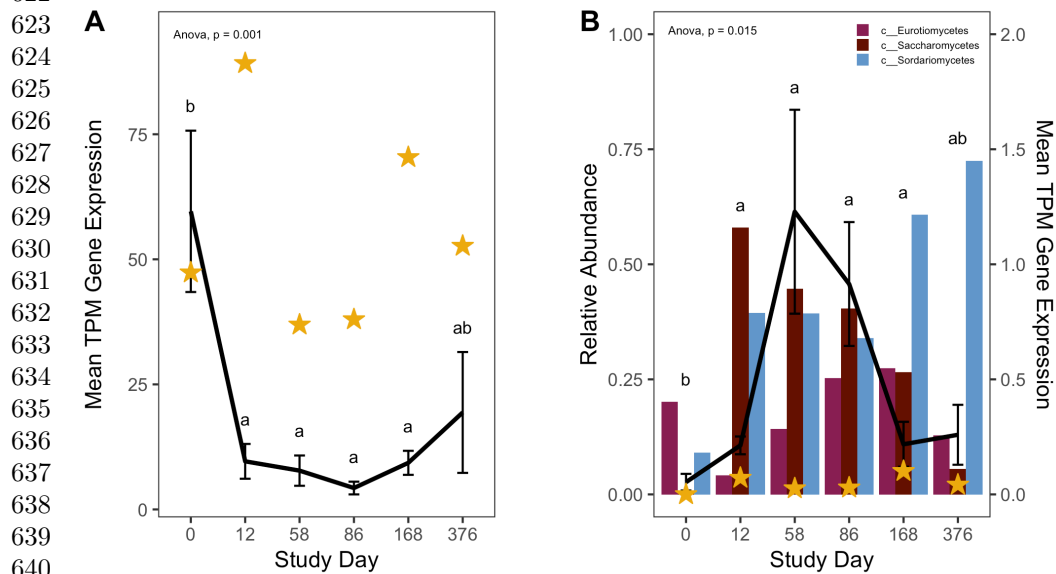
Differential expression comparing study days 86 with 168 and 168 with 376 identified
genes across a variety of functional categories, with many unclassified in the COG
database or with unknown function (Fig 3A). Expression of carbohydrate transport
and metabolism genes associated with *Bacilli* decreased between day 168 and 376.
Acidobacteria transcripts increased in decomposition-impacted soils between study
day 168 and 376, but were not associated with any single COG category (Fig 3B).

Carbon compound metabolism

We expected to observe increased expression of lipid metabolizing genes during active
and advanced decomposition as microbes degraded lipids deposited in the soil [19].

Therefore, we investigated changes in triacylglycerol lipase (enzyme commission number: 3.1.1.3) gene transcription in our soils. Generally, lipase transcripts decreased as decomposition progressed (HLM $F = 6.564$, $p < 0.001$), however we also observed a significant interaction between study day and taxonomic annotation ($F = 8.786$; $p < 0.001$). Specifically, lipase gene transcripts annotated as bacteria decreased with decomposition time ($F = 10.392$; $p = 0.001$), while fungal lipase transcripts increased, reaching a maximum at study day 58 ($F = 4.509$; $p = 0.015$) (Fig 4).

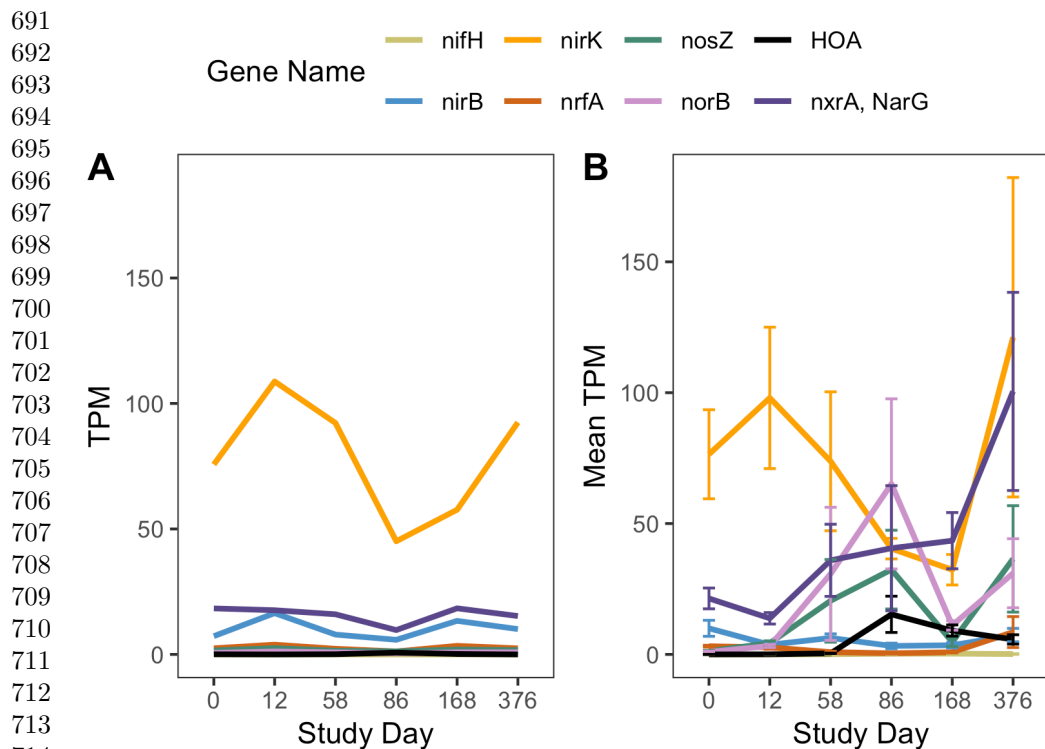
Figure 4: Mean transcript abundance, in transcripts per million (TPM), of all bacterial (A) and fungal (B) triacylglycerol lipase (EC 3.1.1.3) genes over time. Black lines (A, B) report mean and standard deviation of TPM from three individuals (black line), while gold stars denote mean TPM in control soils. P-values are the result of ANOVAs where average TPM and study day are the dependent and independent variables, respectively, while letters are the result of post-hoc Tukey tests between decomposition timepoints. In B, bars show the relative abundance of the fungal classes *Saccharomycetes*, *Sordariomycetes*, and *Eurotiomycetes*, reported in Taylor et al. (2024).



Nitrogen- and sulfur compound transformations

Expression of nitrogen cycling genes was impacted in response to human decomposition. Due to the detection of *hao* in our differential expression analysis, and our hypotheses predicting changes to nitrogen transformation processes, the expression of genes encoding common enzymes involved in nitrogen cycling (*nifH*, *nirB*, *nirK*, *norB*, *nosZ*, *nrfA*, *nrrA*, and *amoA*) were assessed using their enzyme commission numbers (Fig 5A,B). *nifH*, encoding a subunit of nitrogenase which is involved in nitrogen fixation, displayed little to no changes in gene expression between control and decomposition soils. Transcripts for two genes encoding enzymes contributing to the last two steps of denitrification, *norB* (encodes nitric oxide reductase) and *nosZ* (encodes nitrous oxide reductase), increased between study days 12 and 86, and decreased at study day 168 before increasing again at day 376. In contrast, expression of genes encoding nitrate reductase, *narG*, and NO-forming nitrite reductase, *nirK*, remained low until day 376 when transcripts for both genes increased. As noted above, expression of *hao*, encoding hydroxylamine dehydrogenase, increased at study day 86 before decreasing at remaining timepoints (Fig 3A, Fig 5B). Expression of *amoA*, encoding a subunit of ammonia monooxygenase, and *nrrA*, encoding a subunit of nitrite oxidoreductase, which are involved in nitrification, changed in response to decomposition. *amoA* transcripts initially decreased at day 12, remaining reduced until study day 376. Similarly, abundance of genes that encode for enzymes involved in dissimilatory nitrate reduction, *nirB*, and *nrfA*, was low for the first 168 days, with *nrfA* expression increasing at day 376 (Fig 5B).

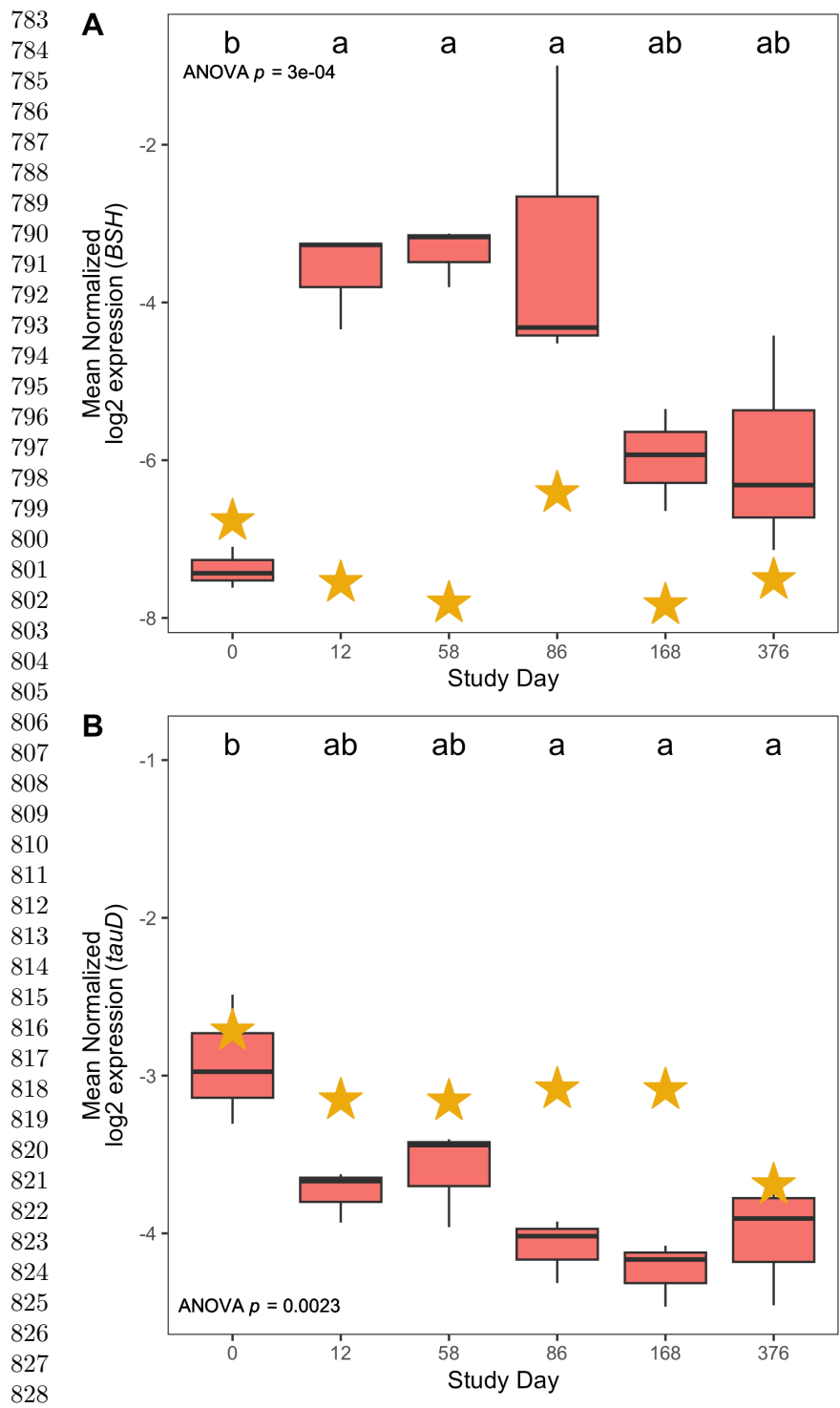
Figure 5: Mean gene expression, in transcripts per million (TPM), of commonly used marker genes for enzymes involved in nitrogen cycling over time in controls (A) and decomposition (B) soils. Data in B represent mean and standard deviation of TPM from three individuals.



Expression of genes involved in metabolism of nitrogen and sulfur-containing compounds were also impacted by human decomposition. Specifically, four of the top ten genes whose expression decreased at day 12 were related to taurine metabolism, with their annotations associated with *tauD*, encoding taurine dioxygenase. (Supplementary Material 6). Further investigation into *tauD* showed that mean expression of these genes decreased steadily over one year, beginning at day 12 (Fig 6B); however, *tauD* expression in response to human decomposition was variable across taxonomic associations. Most *tauD* transcripts were associated with *Gammaproteobacteria*, *Actinobacteria*, *Betaproteobacteria*, *Alphaproteobacteria*, and fungi. While a majority of the *tauD* gene queries displayed reduced expression over time, expression of fungal-associated and a few *Betaproteobacteria*-associated *tauD* genes increased at day 58 (Supplementary Material 7). Sources of taurine in the human body include taurine

absorbed from the diet and taurine produced from anaerobic microbial deconjugation of bile salts via bile salt hydrolase (BSH) enzymes [22]. Therefore, we also looked at expression of genes encoding BSH enzymes in decomposition soils. Expression of these genes was elevated at days 12, 58, and 86 before converging toward pre-decomposition levels at days 168 and 376 (Fig 6A). Hierarchical liner mixed effects (HLM) models showed that both *tauD* (HLM $F = 7.356$, $p = 0.002$) and BSH ($F = 13.768$, $p < 0.001$) gene expression was significantly different over time (Fig 6A,B).

Figure 6: Mean bile salt hydrolase, BSH, (A) and *tauD*, taurine dioxygenase, (B) log2 normalized expression in controls (gold stars) and decomposition (boxplots) soils. Boxplots display the 25th and 75th quartiles and median log2 normalized values between all three individuals at each timepoint. ANOVA p-value is the result of a hierarchical linear mixed effects model accounting for repeated measures of each donor block, while letters denote the results of *post-hoc* Tukey test.



Discussion

The goal of this study was to assess soil microbial gene expression in response to human decomposition. Metatranscriptomics were applied to soil samples collected over one year from below three decomposing human bodies. From this, we found that microbial gene expression shifted over time, with samples reproducible between individuals. Additionally, we showed that gene expression profiles had not recovered to pre-decomposition conditions after one year. Comparison of control and decomposition expression profiles revealed that heat-shock proteins were elevated in response to decomposition. We also described expression patterns between decomposition timepoints, noting changes in functional gene categories at certain timepoints, in particular with respect to lipid, nitrogen and sulfur metabolism.

Decomposition impacted soil community gene expression, even after a year

Gene expression profiles remained altered after one year of decomposition. It is unclear if soil microbial communities, in terms of gene expression profiles, have reached a new steady state as a result of decomposition, or if they would eventually return to pre-decomposition conditions. The soil pH, EC, NH_4^+ , NO_3^- , and total nitrogen (TN) exhibited differences (although not statistical) in these soils following a year of decomposition, however bacterial and fungal community structures, as assessed by rRNA amplicon libraries, were still altered [13]. This indicates that decomposition can continue to structure microbial communities and impact their function for extended periods of time. While nutrient pools and communities both demonstrate less rapid change at later time points in the study, there is not evidence suggesting an arrival at a steady-state post-disturbance microbial community. In some studies, human decomposition can result in elevated carbon and nutrients (organic nitrogen, ammonium, nitrate, and phosphate) for longer than a year [3], suggesting decomposition events

875 have long lasting effects on the local ecosystem. Together, this has implications for
876 terrestrial ecosystem processing (*e.g.*, nutrient cycling, emission of greenhouse gasses,
877 etc.), as we show that decomposition alters functional metabolism pathways within
878 soil microbial communities. Further work with extended sample collections beyond
880 one year are needed to address how long microbial communities and their functions
881 are impacted.
882
883
884

885 Bacteria, fungi, and archaea were all represented in expressed genes throughout
886 decomposition, suggesting that members of all three domains have the potential to
887 contribute to decomposition processes and nutrient cycling. While a majority of anno-
888 tated transcripts were identified as bacteria, fungal transcripts were the second most
889 abundant group. Fungal transcripts made up almost half (seven of the top 15) of the
890 significantly differentially expressed genes associated with decomposition-impacted
891 soils. Additionally, with respect to expression shifts between decomposition time-
892 points, fungal transcripts were among the topmost upregulated genes at study day
893 86. The presence of fungal transcripts is not surprising as fungi are key decomposers,
894 involved in the degradation of organic matter in terrestrial ecosystems [23]. It was
895 interesting to see an increase in certain fungal transcripts, such as lipase, at study
896 days 58 and 86 when soil oxygen began to recover. We would expect lipids to enter
897 the soil as tissues are broken down during decomposition, so we were surprised to
898 see bacterial lipase genes decrease during decomposition. This suggests that microbial
899 activity in decomposition soils may be constrained by the changing chemical environ-
900 ment, potentially altered oxygen levels in the case of bacterial lipase gene expression.
901 Prior work with these soils showed that soil oxygen concentration was a key driver of
902 changes in both bacterial and fungal community composition [13].
903
904
905
906
907
908
909
910
911
912
913
914
915
916
917
918
919
920

Increased stress responses during decomposition	921
	922
Soil microbial communities expressed stress response genes in response to human	923
decomposition. Differential expression analysis identified increased expression of mul-	924
tipl heat shock proteins associated with the taxa <i>Xanthomonadales</i> , <i>Actinobacteria</i> ,	925
and fungi. Upon further investigation, expression of these genes increased through day	926
58 and remained high for the remainder of the year. Soil temperature was elevated rel-	927
ative to controls between study days 8 and 80, with maximum temperatures $>40^{\circ}\text{C}$,	928
while soil electrical conductivity increased up to 663 $\mu\text{S}/\text{cm}$ (16X higher than back-	929
ground) through day 58 before slowly decreasing through the remainder of the study.	930
Soil electrical conductivity (correlates with ionic strength [24] and can indicate soil	931
salinity) has previously been shown to increase in decomposition soils [8–10, 13]. As	932
a result, we would expect these microbes to be experiencing both heat and osmotic	933
stress during this period. Prior work has observed increased heat shock gene expres-	934
sion during salt stress in paddy soils [25] and the presence of both heat and osmotic	935
stress genes in desert soils along a salt gradient [26], suggesting saline conditions can	936
alter the expression of heat and/or osmotic stress genes. In our study we observed	937
that stress response within soil microbial communities is stimulated during human	938
decomposition, however, at this time, it is unclear if expression of these genes is in	939
response to heat stress alone, or in combination with osmotic stress.	940
	941
	942
	943
	944
	945
	946
	947
	948
	949
	950
	951
	952
	953
Increased expression of fungal lipase genes during	954
decomposition	955
	956
	957
Human fat tissue contains lipids that are broken down during decomposition. There-	958
fore, we assessed expression of triacylglycerol lipase genes in decomposition soils. Our	959
results show that expression of triacylglycerol lipase genes was altered in response	960
to decomposition, and these shifts differed between bacterial and fungal transcripts,	961
	962
	963
	964
	965
	966

specifically bacterial triacylglycerol lipase transcripts decreased in response to decomposition, while fungal triacylglycerol lipase transcripts increased. Further, expression of these genes corresponded to changes in relative abundance of the fungal classes *Saccharomycetes*, *Sordariomycetes*, and *Eurotiomycetes* [13]. These fungi have been previously associated with decomposition soils [27, 28] and are known to contain triacylglycerol lipase genes in their genomes [29, 30], suggesting that they play a role in lipid degradation in decomposition soils.

Our observation of an overall decrease in triacylglycerol lipase transcripts contrasts with previous work by Howard et al. (2010) [19], who observed increased gene copy number of Group 1 lipase genes via qPCR during swine decomposition. Fatty acid composition differs in human compared to pig tissue [31], potentially altering the lipid profile available for microbes, leading to differences in decomposition products within the soil [18]. These products can then directly or indirectly alter community composition and/or activity of functional proteins via substrate availability or the chemical environment. Further, decomposition of humans and pigs resulted in increased pH in soils below pigs, and decreased pH below humans [18]. Altered pH and soil chemistry could result in a different functional potential and/or gene expression in decomposition-impacted soils. Many triacylglycerol lipases have a pH optimum that is neutral to basic [32–34], so cells may be decreasing expression under acidic conditions in human decomposition soils. Availability of lipid species and changes to pH may select for taxa that favor these substrates/pH conditions; for example, Mason et al. (2022) [12] suggested the abundance of the fungal taxa *Saccharomycetes* was related to antemortem BMI due to relative proportions of fat and muscle tissue.

Evidence for phased denitrification and nitrification

The human body is a concentrated source of nitrogen that is released into the surrounding soil during decomposition, therefore we also evaluated expression of genes involved

in nitrogen cycling. Expression of common marker genes for nitrogen cycling was altered in decomposition soil and suggested nitrogen transformations during human decomposition are driven by soil oxygen concentrations with hydroxylamine as an important intermediate. We observed low or reduced expression of nitrification genes *nrrA* and *amoA* between days 12 and 86, during a period when oxygen was reduced to 39% - 85%. This was concomitant with accumulation of ammonium, which reached a maximum on day 12, and low nitrate conditions indicating that nitrification was inhibited. This period of reduced soil oxygen constraining nitrification was also described in a decomposition experiment with beaver carcasses Keenan et al. (2018) [8].

We observed increased expression of *hao*, which encodes the enzyme hydroxylamine dehydrogenase (HAO) at day 86 while oxygen was reduced (~85%). This corresponded to simultaneous increases in expression of genes encoding nitric oxide reductase (*norB*) and nitrous oxide reductase (*nosZ*). Traditionally HAO has been thought to process hydroxylamine to nitrite during nitrification, while NorB and NosZ are enzymes involved in the last two steps of denitrification converting nitric oxide (NO) to dinitrogen gas (N₂). However, recent work has suggested hydroxylamine can be converted to nitric oxide (NO), as well as can interact with multiple phases of the nitrogen cycle [35]. Even though *amoA* expression was shown to decrease during reduced oxygen conditions, *amoA* transcripts were still present and likely able to convert ammonium to hydroxylamine as soil oxygen was not completely depleted during decomposition. Additionally, a previous study reported that the growth of the ammonia oxidizing bacteria *Nitrosomonas europaea* under anoxic conditions lead to accumulation of hydroxylamine in a chemostat bioreactor [36], suggesting anaerobic ammonium oxidation (anammox) may also be occurring in decomposition soils. However, we did not observe increases in *nirK* expression, which might suggest conversion of nitrite to NO for use in the anammox pathway. NO produced via HAO activity may be used for anammox in these soils; however, the role of hydroxylamine as an intermediate

in anammox is still debated [35]. Therefore, our current hypothesis is that hydroxylamine accumulates under anaerobic conditions during decomposition, which can then be converted to NO by HAO. This NO would then be present for anaerobic denitrifying bacteria to convert to nitrous oxide (N₂O) by NorB and finally to N₂ by NosZ. Keenan et al. (2018) [8] also noted a brief increase in N₂O emissions, which suggests denitrification was occurring during this phase of reduced soil oxygen concentrations. As soils fully reoxygenated by day 168, we observed increased expression of genes encoding enzymes involved in aerobic nitrification, *amoA* and *nxrR*. Nitrification is an oxygen-dependent process which would be converting the accumulated ammonium to nitrate; the increase in nitrate concentrations may then serve as a substrate for denitrification. We observed increased expression of marker genes encoding all four enzymes in the complete dissimilatory denitrification pathway (*narG*, *nirK*, *norB*, and *nosZ*) at day 376. Increased expression of nitrification and denitrification marker genes is consistent with accumulation of nitrite, nitrate, and N₂O after oxygen is reintroduced to soils described in Keenan et al. (2018) [3, 8]. Together, gene expression patterns in our study provide further insight into nitrogen transformations in during vertebrate decomposition, suggesting an important role of hydroxylamine.

Increased expression of bile salt hydrolases

Sulfur is present in various organic molecules, including taurine, a sulfur- and nitrogen-containing acid involved in bile acid formation [22]. Taurine is present in the human body, where it can be absorbed from the diet or synthesized in the liver [37]. However, taurine is also produced as a byproduct of the deconjugation of bile salts via bile salt hydrolases (BSH) present in the anaerobic gut taxa *Lactobacillus* and *Clostridium* [22]. In our study, we observed increased expression of genes encoding BSH enzymes between days 12 and 86. Given that increased expression of BSH genes corresponded to the beginning of active decomposition, when decomposition products were observed

to enter the soil, and the period of reduced dissolved oxygen in our study, it is likely that taurine accumulation is the result of BSH enzyme activity by anaerobic microorganisms. While we did not measure taurine concentrations in this study, our results correspond to previous decomposition studies that report accumulation of taurine in various organs and body regions [38–40] and soils [18, 41] during decomposition via metabolomics, and increased relative abundance of *Clostridium* and *Lactobacillus* within the body [42–44] and in decomposition soils [20] via DNA sequencing methods, including in these soils [13].

One pathway of taurine metabolism is through desulfurization via the α -ketoglutarate-dependent enzyme taurine dioxygenase (TauD). Specifically, this enzyme, encoded by the gene *tauD*, converts 2-oxoglutarate and taurine to produce aminoacetaldehyde, succinate, sulfite, and CO₂ [45]. Succinate and sulfite from this reaction can then be used for the citric acid cycle and sulfur metabolism, respectively. Given increased BSH expression in our study and reported taurine accumulation in others, we would expect taurine to be present for microbial metabolism by TauD. However, we observed a general decrease in *tauD* expression between days 12 through 376. This trend was driven by reduced expression of *tauD* transcripts associated with *Proteobacteria*, *Gammaproteobacteria*, and *Actinobacteria* whose relative abundance have been shown to remain consistent or increase during human decomposition [20], suggesting that *tauD* expression is downregulated under decomposition conditions. However, we noted that expression of *tauD* genes associated with fungi and a few *Betaproteobacteria* displayed increased expression at day 58, corresponding to increased expression of bile salt hydrolases (BSH) between days 12 and 86. The reduction in *tauD* expression may be due to increased sulfur availability. We did not measure sulfur species in this experiment; however, others have observed increased sulfur concentrations in decomposition-impacted soils [3, 7, 11]. Thus, sulfur scavenging pathways such as taurine desulfurization by TauD [46], whose genes are expressed under sulfur-limiting

1151 conditions, likely display reduced expression under sulfur replete conditions. Addition-
1152 ally, taurine may be processed through other pathways. For example, taurine can be
1153 deaminated by taurine dehydrogenase to produce sulfite and acetyl-CoA for carbon
1154 metabolism [45, 47]. Overall, our results suggest that human decomposition has poten-
1155 tial impacts on soil sulfur biogeochemistry through deposition of inorganic (sulfate)
1156 and organic (sulfur-containing amino acids) sulfur compounds.
1157
1158
1159
1160

1161 1162 **Conclusion** 1163

1164
1165 This study investigated soil microbial gene expression during human decomposition.
1166 Metatranscriptomic analysis of soils from three human individuals over one year shows
1167 that decomposition impacted microbial community gene expression profiles, exhibit-
1168 ing functional shifts over time. This included altered expression of genes involved in
1169 lipid, N and S metabolism as microbes processed the nutrient-rich tissues of the human
1170 body. Additionally, we noted that functionality within decomposition-impacted soils
1171 was still affected after one year and had not returned to starting or background condi-
1172 tions. Together, these results show that vertebrate decomposition has lasting impacts
1173 on local soil ecosystems, including soil microbial communities. These results have
1174 important implications for understanding biogeochemical changes due to vertebrate
1175 mortality events in terrestrial ecosystems.
1176
1177
1178
1179
1180
1181
1182

1183 1184 **Materials and Methods** 1185

1186 1187 **Study design** 1188

1189 In February 2018, three deceased male human subjects (hereafter, “donors”) were
1190 placed supine on the soil surface at the University of Tennessee Anthropology Research
1191 Facility (ARF) and allowed to decompose. Located in Knoxville, TN (35° 56’ 28” N,
1192 83° 56’ 25” W) the ARF is a roughly 2-acre outdoor facility dedicated to studying
1193
1194
1195
1196

human decomposition [48]. The soils at the ARF are comprised of the Loyston-Talbott Rock outcrop (LtD) and Coghill-Corryton (CcD) complexes. LtD soils are a silty clay loam and channery clay overlaying lithic bedrock, while CcD soils are comprised of clay from weathered quartz limestone [13, 48]. A site that had not been previously exposed to decomposition was used for this study.

The decomposition field experiment is fully described in Taylor et al. (2024) [13]. Briefly, experiments were conducted in a block design, where each block consisted of one decomposition site and one control site [13]. In total three blocks, *i.e.*, three donors paired with three respective control sites, were included in the study. Each control site was chosen in a manner to ensure their location was uphill and roughly 2 m away from decomposition sites [13]. Donor internal temperatures were recorded by probes located in the abdomen, while ambient air temperatures were monitored via sensors located roughly 50 cm above the soil surface. Soil temperature and salinity were measured with sensors placed directly underneath each individual (Decagon Devices, GS3) [13]. Donor ages ranged from 65 to 86 and were within 1 kg of each other with regard to weight (90.7 to 91.6 kg); donor BMI varied between 27.7 to 29.6 [13].

Sampling and physiochemistry

Decomposition of all subjects was observed for one year. During the one-year study period, soils were sampled at 20 timepoints chosen to correspond with morphological stages of decomposition as described by [49]. Once advanced decay was reached, soils were collected at intervals of 350 accumulated degree days (ADD), calculated using ambient air temperatures, up to one year. All soil cores were taken using a 1.9 cm (3/4 inch) diameter soil auger to a depth of 16 cm. Soils were divided into two depth fractions: 0-1 cm (interface) and 1-16 cm (core) for the analyses reported in Taylor et al. (2024) [13]; the entire 0 to 16 cm core was used for this current study. Decomposition soils were taken from directly beneath the cadavers, taking care to not re-sample

1243 the same location more than once. At the time of sampling, soil dissolved oxygen was
 1244 measured in triplicate using an Orion Star™ A329 pH/ISE/Conductivity/Dissolved
 1245 Oxygen portable multiparameter meter (ThermoFisher) [13].
 1246
 1247
 1248 A subset of 6 study timepoints were chosen for metatranscriptomics analysis. Study
 1249 days 0, 12, 58, 86, 168, and 376 were chosen as they represented distinct morphologi-
 1250 cal and soil biogeochemical stages during decomposition. Study day 0 was chosen as
 1251 a baseline sample prior to cadaver placement. Study day 12 was the start of active
 1252 decomposition and corresponded to maximum soil ammonium concentrations and
 1253 minimum soil oxygen (approximately 39%). Study day 58 was chosen as this sample
 1254 represented the pH minimum, and respiration and soil temperature were at a maxi-
 1255 mum [13]. Additionally, ammonium concentrations began to decrease around day 58.
 1256 Study day 86 was when soil oxygen started to recover and nitrate levels began to
 1257 increase. Study day 168 was chosen as nitrate was at its maximum and soil dissolved
 1258 oxygen had returned to 99%. Finally, day 376 was chosen to represent the end of the
 1259 study, 1 year since cadaver placement. Each study day was represented by four soil
 1260 samples for RNA extraction: one pooled control sample which was a mix of the three
 1261 control locations, plus one sample from each of the three donors, yielding a total of
 1262 24 samples for this study.
 1263
 1264 Soil samples were transported back to the University of Tennessee (Knoxville, TN)
 1265 and processed within 24 hours of collection. Soils were homogenized by hand to remove
 1266 insect larvae, roots, rocks, and other debris (> 2 mm). A subset of soils were used
 1267 to measure pH, electrical conductivity (EC), and evolved CO_2 as described in Taylor
 1268 (2024). Soil nitrogen species (NH_4^+ , NO_3^-) and total carbon (TC) and nitrogen (TN)
 1269 were measured in all soil samples as described in [13]. Reported values for soil phys-
 1270 iochemistry represent the full 16 cm core; estimated by summing interface and core
 1271
 1272
 1273
 1274
 1275
 1276
 1277
 1278
 1279
 1280
 1281
 1282
 1283
 1284
 1285
 1286
 1287
 1288

values reported by Taylor et. al, (2024) [13] in 1:16 and 15:16 ratios, respectively. Control reported here are means of the three experimental controls that were unimpacted by decomposition.

Roughly 10 g of soil was reserved for nucleic acid extraction, placed in a 4 oz. Whirl-Pak™ bag (Nasco), and flash frozen in liquid nitrogen. All samples were stored at -80°C until further analysis. Bacterial and fungal community composition was assessed via amplicon sequencing of the 16S rRNA gene and ITS2 region as described in Taylor et al. (2024).

RNA Extraction and Sequencing

RNA was extracted from 2 g of soil using Qiagen's RNeasy® PowerSoil® Total RNA kit. Manufacturer's instructions were followed with a few modifications. Soils became saline during decomposition; therefore, we followed the manufacturer's suggestion and incubated all extracts at -20°C following addition of solution SR4 (step 9) to decrease salt precipitation. All RNA samples were resuspended in 40 µl of Solution SR7. RNA concentrations were assessed fluorometrically using the Qubit® RNA HS assay (catalog no. Q32852) with 1 µl of RNA. DNA contamination was removed by DNase treating RNA extracts twice using Qiagen's DNase Max® kit in 50 µl reactions. RNA concentrations were remeasured after DNase treatment. PCR with V4 16S rRNA gene primers [50, 51] was conducted using RNA extracts as the template to confirm removal of all DNA prior to sequencing. RNA aliquots were shipped to HudsonAlpha Discovery (Huntsville, AL) for library preparation and RNA sequencing. Dual-indexed libraries were prepared using the Illumina® Stranded Total RNA prep with ribosomal RNA depletion via ligation with Ribo-Zero Plus. Libraries were then pooled and sequenced on Illumina's NovaSeq 6000 v4 platform, resulting in demultiplexed fastq files for each sample.

1335 Bioinformatics

1336

1337 Illumina sequencing of the 24 libraries yielded a total of 5,073,476,730 reads, or
1338
1339 2,536,738,365 paired reads, with a mean of 105,697,432 paired reads per sample. Read
1340
1341 quality control (QC) was conducted in KBase [52] using Trimmomatic [53]. Paired
1342
1343 fastq files were imported to KBase through Globus. Poor quality reads were removed
1344 (4.7% of all reads), and adapters trimmed via Trimmomatic (v0.36) using default set-
1345
1346 tings and the TruSeq3-PE-2 adapter file, resulting in 4,834,123,062 total reads. After
1347
1348 QC check with FastQC, trimmed libraries were exported as fastq files from KBase
1349
1350 through Globus. Remaining ribosomal RNA was filtered using bbmap (maxindel =
1351
1352 20, minid = 0.93) from the Joint Genome Institute's (JGI) bbttools suite [54]. Fil-
1353
1354 tering of ribosomal RNA further removed 7.3% of reads, leaving 4,479,804,360 reads
1355
1356 for assembly. Following this step, all non-ribosomal reads from all 24 samples were
1357
1358 merged into one file. Reads were then co-assembled into contigs using the de novo
1359
1360 assembler MEGAHIT (v1.2.9) [55] (-12 -k-min 23, -k-max 123, -k-step 10).

1358

1359
1360 Gene identification and annotation from co-assembled contigs was performed using
1361
1362 Prodigal [56] and eggNOG mapper [57], respectively. Briefly, the fastq containing all
1363
1364 contigs was submitted to Prodigal (v2.6.3) for protein coding gene predication for a
1365
1366 meta-sample (-p meta -f gff). After co-assembly, a total of 6,257,674 proteins were
1367
1368 identified by Prodigal. Next, predicated genes were functionally and taxonomically
1369
1370 annotated using eggNOG mapper (v2.1.6) using basic settings to perform a diamond
1371
1372 blastp search [58]. From this, 1,048,573 proteins were annotated by eggNOG-mapper
1373
1374 (16.7%). Most of the annotated proteins were taxonomically annotated as bacteria
1375
1376 (91.3%), followed by eukaryotes (7.6 %), and archaea (0.81 %). Of the 7.6% of eukary-
1377
1378 otic proteins, 64.4% (4.9% of all proteins) were annotated as fungi. For this study,
1379
1380 genes of interest included all bacterial, archaeal, and fungal proteins, therefore all
1381
1382 non-fungal eukaryotic proteins (32,004) were removed prior to downstream analysis.
1383
1384 Transcript counts for all genes of interest were obtained by mapping reads from each

respective sample to genes of interest obtained from co-assembly using QIAGEN CLC Genomics Workbench 20.0 (<https://digitalinsights.qiagen.com/>). The percent of reads mapped to genes of interest ranged from 21% to 38% between samples, with an average of 31% reads mapped. Gene counts were then combined in a single file and used for downstream analyses in R.

Differential Expression

Transcript counts from all samples were combined in a single workable data file and imported into R for differential expression analysis using the R packages edgeR [59] and limma [60] following a modified pipeline by Phipson et al. (2020) [61]. The transcript count table was imported into R and converted to a DGElist object. Genes without sufficient counts for statistical analysis were removed to increase power using the edgeR function filterByExpr(), using study day as the comparison group.

Raw counts were then log2 normalized and gene expression profiles compared via multidimensional scaling (MDS) and hierarchical clustering. Multidimensional scaling (MDS) was conducted using plotMDS() from the limma package to assess differences between samples. MDS values were extracted from the MDS object, and the first two dimensions plotted using ggplot2 [62]. We also assessed the relationship between gene expression profiles and changes in the soil environment using canonical correspondence analysis (CCA). Environmental variables of interest included decomposition time in accumulated degree hours (ADH) based on ambient temperatures, ADH based on internal gut temperatures, ADH based on soil temperatures, gravimetric moisture, pH, electrical conductivity (EC), dissolved oxygen (DO), CO₂ (mol gdw⁻¹), NH₄ (mg gdw⁻¹), NO₃ (mg gdw⁻¹), N %, C %, and CN ratio. First, permutational multivariate analysis of variance (PERMANOVA) with adonis() (vegan v2.6.7) [63] was used to identify significant soil parameters. Then the vegan functions cca() and scores() were

1427 applied to run the CCA and extract scores, respectively. Scores for the first two
1428 dimension were plotted using ggplot2, with loadings extracted from the CCA biplot.
1429
1430
1431 For differential expression analysis, raw filtered reads were normalized using edgeR's
1432 trimmed mean of M values (TMM) normalization using the function calcNormFac-
1433 tors(). TMM normalized reads were then log2 transformed using limma's voom() and
1434 differential expression assessed. Empirical Bayes shrinkage was used correct to p-
1435 values for false discovery rates. The topmost up and down regulated genes for each
1436 comparison, determined by log2 fold change and adjusted p-values, were then reported.
1437
1438
1439
1440 Expression of certain genes were assessed after performing transcripts per million
1441 (TPM) normalization and statistical analyses with a combination of analysis of vari-
1442 ance (ANOVA) and post-hoc Tukey tests. ANOVA across all timepoints were applied
1443 to hierarchical linear mixed effects models to account for repeated sampling within
1444 each donor block.
1445
1446
1447
1448
1449
1450

1451 **Data availability**

1452
1453 Raw RNA sequence files from the Illumina Novaseq are available at the National Cen-
1454 ter for Biotechnology Information's (NCBI) Sequence Read Archive (SRA) as a part
1455 of [BioProject PRJNA1066312](#) under BioSample accession numbers SAMN45195141-
1456 SAMN45195164. Additional datasets supporting the conclusions of this article are
1457 available on [GitHub](#).
1458
1459
1460
1461
1462

1463 **Code availability**

1464
1465 The code used for analysis and to generate figures are available on [GitHub](#).
1466
1467
1468
1469
1470
1471
1472

References

- [1] Benninger, L. A., Carter, D. O. & Forbes, S. L. The biochemical alteration of soil beneath a decomposing carcass. *Forensic Science International* **180**, 70–5 (2008).
- [2] Towne, E. G. Prairie vegetation and soil nutrient responses to ungulate carcasses. *Oecologia* **122**, 232–239 (2000). URL <https://doi.org/10.1007/PL00008851>.
- [3] DeBruyn, J. M., Keenan, S. W. & Taylor, L. S. From carrion to soil: microbial recycling of animal carcasses. *Trends in Microbiology* (2024). URL <https://doi.org/10.1016/j.tim.2024.09.003>. Publisher: Elsevier.
- [4] Parmenter, R. R. & MacMahon, J. A. Carrion decomposition and nutrient cycling in a semiarid shrub–steppe ecosystem. *Ecological Monographs* **79**, 637–661 (2009).
- [5] Macdonald, B. C. T. *et al.* Carrion decomposition causes large and lasting effects on soil amino acid and peptide flux. *Soil Biology and Biochemistry* **69**, 132–140 (2014).
- [6] Bump, J. K. *et al.* Ungulate carcasses perforate ecological filters and create biogeochemical hotspots in forest herbaceous layers allowing trees a competitive advantage. *Ecosystems* **12**, 996–1007 (2009).
- [7] Aitkenhead-Peterson, J. A., Owings, C. G., Alexander, M. B., Larison, N. & Bytheway, J. A. Mapping the lateral extent of human cadaver decomposition with soil chemistry. *Forensic Science International* **216**, 127–34 (2012).
- [8] Keenan, S. W., Schaeffer, S. M., Jin, V. L. & DeBruyn, J. M. Mortality hotspots: nitrogen cycling in forest soils during vertebrate decomposition. *Soil Biology and Biochemistry* **121**, 165–176 (2018).

1473
1474
1475
1476
1477
1478
1479
1480
1481
1482
1483
1484
1485
1486
1487
1488
1489
1490
1491
1492
1493
1494
1495
1496
1497
1498
1499
1500
1501
1502
1503
1504
1505
1506
1507
1508
1509
1510
1511
1512
1513
1514
1515
1516
1517
1518

1519 [9] Fancher, J. P. *et al.* An evaluation of soil chemistry in human cadaver decom-
1520 position islands: Potential for estimating postmortem interval (PMI). *Forensic*
1521 *Science International* **279**, 130–139 (2017).
1522
1523
1524
1525 [10] Quaggiotto, M.-M., Evans, M. J., Higgins, A., Strong, C. & Barton, P. S.
1526 Dynamic soil nutrient and moisture changes under decomposing vertebrate
1527 carcasses. *Biogeochemistry* **146**, 71–82 (2019).
1528
1529
1530
1531 [11] Taylor, L. S. *et al.* Soil elemental changes during human decomposition.
1532 *PLoS ONE* **18**, 1–24 (2023). URL <https://doi.org/10.1371/journal.pone.0287094>.
1533 Publisher: Public Library of Science.
1534
1535
1536 [12] Mason, A. R. *et al.* Body mass index (BMI) impacts soil chemical and microbial
1537 response to human decomposition. *mSphere* e0032522 (2022).
1538
1539
1540
1541 [13] Taylor, L. S. *et al.* Transient hypoxia drives soil microbial community dynamics
1542 and biogeochemistry during human decomposition. *FEMS Microbiology Ecology*
1543 **100**, fae119 (2024). URL <https://doi.org/10.1093/femsec/fae119>.
1544
1545
1546 [14] Keenan, S. W., Emmons, A. L. & DeBruyn, J. M. Microbial community coa-
1547 lesence and nitrogen cycling in simulated mortality decomposition hotspots.
1548 *Ecological Processes* **12**, 45 (2023). URL [https://doi.org/10.1186/s13717-023-](https://doi.org/10.1186/s13717-023-00451-y)
1549 [00451-y](https://doi.org/10.1186/s13717-023-00451-y).
1550
1551
1552
1553
1554 [15] Mason, A. R., Taylor, L. S. & DeBruyn, J. M. Microbial ecology of vertebrate
1555 decomposition in terrestrial ecosystems. *FEMS Microbiology Ecology* **99**, fiad006
1556 (2023). URL <https://doi.org/10.1093/femsec/fiad006>.
1557
1558
1559
1560 [16] Burcham, Z. M. *et al.* Total RNA analysis of bacterial community structural
1561 and functional shifts throughout vertebrate decomposition. *Journal of Forensic*
1562 *Sciences* **64**, 1707–1719 (2019).
1563
1564

- [17] Ashe, E. C., Comeau, A. M., Zejdlik, K. & O'Connell, S. P. Characterization of bacterial community dynamics of the human mouth throughout decomposition via metagenomic, metatranscriptomic, and culturing techniques. *Frontiers in Microbiology* **12**, 689493 (2021).
- [18] DeBruyn, J. M. *et al.* Comparative decomposition of humans and pigs: soil biogeochemistry, microbial activity and metabolomic profiles. *Frontiers in Microbiology* **11**, 608856 (2021).
- [19] Howard, G. T., Duos, B. & Watson-Horzelski, E. J. Characterization of the soil microbial community associated with the decomposition of a swine carcass. *International Biodeterioration & Biodegradation* **64**, 300–304 (2010).
- [20] Cobaugh, K. L., Schaeffer, S. M. & DeBruyn, J. M. Functional and structural succession of soil microbial communities below decomposing human cadavers. *Plos One* **10**, e0130201 (2015).
- [21] Singh, B. *et al.* Temporal and spatial impact of human cadaver decomposition on soil bacterial and arthropod community structure and function. *Frontiers in Microbiology* **8**, 2616 (2018).
- [22] Urdaneta, V. & Casadesús, J. Interactions between Bacteria and Bile Salts in the Gastrointestinal and Hepatobiliary Tracts. *Frontiers in Medicine* **4** (2017).
- [23] van der Wal, A., Geydan, T. D., Kuyper, T. W. & de Boer, W. A thready affair: linking fungal diversity and community dynamics to terrestrial decomposition processes. *FEMS Microbiology Reviews* **37**, 477–494 (2013).
- [24] Essington, M. E. *Soil and water chemistry: an integrative approach* (CRC press, 2015).

1611 [25] Peng, J., Wegner, C.-E. & Liesack, W. Short-term exposure of paddy soil micro-
1612 bial communities to salt stress triggers different transcriptional responses of key
1613 taxonomic groups. *Frontiers in Microbiology* **8** (2017).
1614
1615
1616
1617 [26] Pandit, A. S. *et al.* A snapshot of microbial communities from the Kutch: one of
1618 the largest salt deserts in the World. *Extremophiles* **19**, 973–987 (2015).
1619
1620
1621 [27] Metcalf, J. L. *et al.* Microbial community assembly and metabolic function during
1622 mammalian corpse decomposition. *Science* **351**, 158–62 (2016).
1623
1624
1625 [28] Fu, X. *et al.* Fungal succession during mammalian cadaver decomposition and
1626 potential forensic implications. *Scientific Reports* **9**, 12907 (2019).
1627
1628
1629 [29] Dujon, B. *et al.* Genome evolution in yeasts. *Nature* **430**, 35–44 (2004).
1630
1631
1632 [30] Haridas, S. *et al.* The genome and transcriptome of the pine saprophyte *Ophios-*
1633 *toma piceae*, and a comparison with the bark beetle-associated pine pathogen
1634 *Grosmannia clavigera*. *BMC Genomics* **14**, 373 (2013).
1635
1636
1637 [31] Notter, S. J., Stuart, B. H., Rowe, R. & Langlois, N. The initial changes of fat
1638 deposits during the decomposition of human and pig remains. *Journal of Forensic*
1639 *Sciences* **54**, 195–201 (2009).
1640
1641
1642
1643 [32] Kok, R. G. *et al.* Characterization of the extracellular lipase, LipA, of *Acineto-*
1644 *bacter calcoaceticus* BD413 and sequence analysis of the cloned structural gene.
1645 *Molecular Microbiology* **15**, 803–818 (1995).
1646
1647
1648
1649 [33] Hasan, F., Shah, A. A. & Hameed, A. Influence of culture conditions on lipase
1650 production by *Bacillus* sp. FH5. *Annals of Microbiology* **56**, 247–252 (2006).
1651
1652
1653 [34] Zouaoui, B. & Bouziane, A. Production, optimization and characterization of
1654 the lipase from *Pseudomonas aeruginosa*. *Romanian biotechnological letters* **17**,
1655
1656

- 7187–7193 (2012). 1657
- [35] Soler-Jofra, A., Pérez, J. & van Loosdrecht, M. C. M. Hydroxylamine and the 1658
nitrogen cycle: A review. *Water Research* **190**, 116723 (2021). 1659
1660
1661
1662
1663
- [36] Yu, R., Perez-Garcia, O., Lu, H. & Chandran, K. Nitrosomonas europaea adapta- 1664
tion to anoxic-oxic cycling: Insights from transcription analysis, proteomics and 1665
metabolic network modeling. *Science of the Total Environment* **615**, 1566–1573 1666
(2018). 1667
1668
1669
1670
- [37] Seidel, U., Huebbe, P. & Rimbach, G. Taurine: A regulator of cellular redox 1671
homeostasis and skeletal muscle function. *Molecular Nutrition & Food Research* 1672
63, 1800569 (2019). 1673
1674
1675
1676
- [38] Mora-Ortiz, M., Trichard, M., Oregioni, A. & Claus, S. P. Thanatometabolomics: 1677
introducing NMR-based metabolomics to identify metabolic biomarkers of the 1678
time of death. *Metabolomics* **15**, 37 (2019). 1679
1680
1681
1682
- [39] Locci, E. *et al.* A ¹H NMR metabolomic approach for the estimation of the time 1683
since death using aqueous humour: an animal model. *Metabolomics* **15**, 76 (2019). 1684
1685
1686
- [40] Zelentsova, E. A. *et al.* Post-mortem changes in the metabolomic compositions 1687
of rabbit blood, aqueous and vitreous humors. *Metabolomics* **12**, 172 (2016). 1688
1689
1690
- [41] Hoeland Katharina, M. *Investigating the potential of postmortem metabolomics 1691
in mammalian decomposition studies in outdoor settings*. Ph.D. thesis, University 1692
of Tennessee-Knoxville, https://trace.tennessee.edu/utk_graddiss/7000 (2021). 1693
1694
1695
1696
- [42] Javan, G. T. *et al.* Human thanatomicrobiome succession and time since death. 1697
Scientific Reports **6**, 29598 (2016). 1698
1699
1700
1701
1702

1703 [43] Javan, G. T., Finley, S. J., Smith, T., Miller, J. & Wilkinson, J. E. Cadaver
1704 thanatomicrobiome signatures: the ubiquitous nature of *Clostridium* species in
1705 human decomposition. *Frontiers in Microbiology* **8**, 2096 (2017).
1706
1707
1708
1709 [44] DeBruyn, J. M. & Hauther, K. A. Postmortem succession of gut microbial
1710 communities in deceased human subjects. *Peerj* **5**, e3437 (2017).
1711
1712
1713 [45] Cook, A. M. & Denger, K. Metabolism of taurine in microorganisms. *Taurine* **6**
1714 3–13 (2006).
1715
1716
1717 [46] Kertesz, M. A. Riding the sulfur cycle – metabolism of sulfonates and sul-
1718 fate esters in Gram-negative bacteria. *FEMS Microbiology Reviews* **24**, 135–175
1719 (2000).
1720
1721
1722
1723 [47] Brüggemann, C., Denger, K., Cook, A. M. & Ruff, J. Enzymes and genes of
1724 taurine and isethionate dissimilation in *Paracoccus denitrificans*. *Microbiology*
1725 (*Reading, England*) **150**, 805–816 (2004).
1726
1727
1728
1729 [48] Keenan, S. W. *et al.* Spatial impacts of a multi-individual grave on microbial
1730 and microfaunal communities and soil biogeochemistry. *PLoS One* **13**, e0208845
1731 (2018).
1732
1733
1734
1735 [49] Payne, J. A. A summer carrion study of the baby pig *Sus Scrofa* Linnaeus.
1736 *Ecology* **46**, 592–602 (1965).
1737
1738
1739 [50] Apprill, A., McNally, S., Parsons, R. & Weber, L. Minor revision to V4 region SSU
1740 rRNA 806R gene primer greatly increases detection of SAR11 bacterioplankton.
1741 *Aquatic Microbial Ecology* **75**, 129–137 (2015).
1742
1743
1744
1745 [51] Parada, A. E., Needham, D. M. & Fuhrman, J. A. Every base matters: assessing
1746 small subunit rRNA primers for marine microbiomes with mock communities,
1747
1748

time series and global field samples. *Environmental Microbiology* **18**, 1403–14 (2016).

[52] Arkin, A. P. *et al.* KBase: The United States Department of Energy Systems Biology Knowledgebase. *Nature Biotechnology* **36**, 566–569 (2018).

[53] Bolger, A. M., Lohse, M. & Usadel, B. Trimmomatic: a flexible trimmer for Illumina sequence data. *Bioinformatics* **30**, 2114–2120 (2014).

[54] Bushnell, B. BBMap. URL sourceforge.net/projects/bbmap/.

[55] Li, D., Liu, C.-M., Luo, R., Sadakane, K. & Lam, T.-W. MEGAHIT: an ultra-fast single-node solution for large and complex metagenomics assembly via succinct de Bruijn graph. *Bioinformatics* **31**, 1674–1676 (2015).

[56] Hyatt, D. *et al.* Prodigal: prokaryotic gene recognition and translation initiation site identification. *BMC Bioinformatics* **11**, 119 (2010).

[57] Cantalapiedra, C. P., Hernández-Plaza, A., Letunic, I., Bork, P. & Huerta-Cepas, J. eggNOG-mapper v2: functional annotation, orthology assignments, and domain prediction at the metagenomic scale. *Molecular Biology and Evolution* **38**, 5825–5829 (2021).

[58] Buchfink, B., Reuter, K. & Drost, H.-G. Sensitive protein alignments at tree-of-life scale using DIAMOND. *Nature Methods* **18**, 366–368 (2021).

[59] Robinson, M. D., McCarthy, D. J. & Smyth, G. K. edgeR: a Bioconductor package for differential expression analysis of digital gene expression data. *Bioinformatics* **26**, 139–140 (2010).

[60] Smyth, G. K. in *limma: Linear Models for Microarray Data* (eds Gentleman, R., Carey, V. J., Huber, W., Irizarry, R. A. & Dudoit, S.) *Bioinformatics and*

1795 *Computational Biology Solutions Using R and Bioconductor* 397–420 (Springer
1796 New York, New York, NY, 2005).

1798
1799 [61] Phipson, B. *et al.* Differential expression analysis (2020). URL [https://combine-](https://combine-australia.github.io/RNAseq-R/06-rnaseq-day1.html#References)
1800 [australia.github.io/RNAseq-R/06-rnaseq-day1.html#References](https://combine-australia.github.io/RNAseq-R/06-rnaseq-day1.html#References).

1802
1803 [62] Wickham, H. *ggplot2: Elegant Graphics for Data Analysis* (Springer-Verlag New
1804 York, 2016). URL <https://ggplot2.tidyverse.org>.

1806
1807 [63] Oksanen, J. *et al.* *vegan: Community Ecology Package* (2024). URL [https://](https://vegandevs.github.io/vegan/)
1808 vegandevs.github.io/vegan/.

1810
1811

1812 Acknowledgements

1813
1814

1815 We would like to thank the Forensic Anthropology Center at the University of
1816 Tennessee-Knoxville for their help in setting up field experiments. We would like to
1817 thank Mary Davis for her help in managing the field site and helping to obtain donors
1818 for this work. This research was funded by a National Institute of Justice Award
1819 (DOJ-NIJ-2017-R2-CX-0008) to LST and JMD.

1822
1823

1824 Supplementary Information

1825
1826

1827
1828

1829
1830

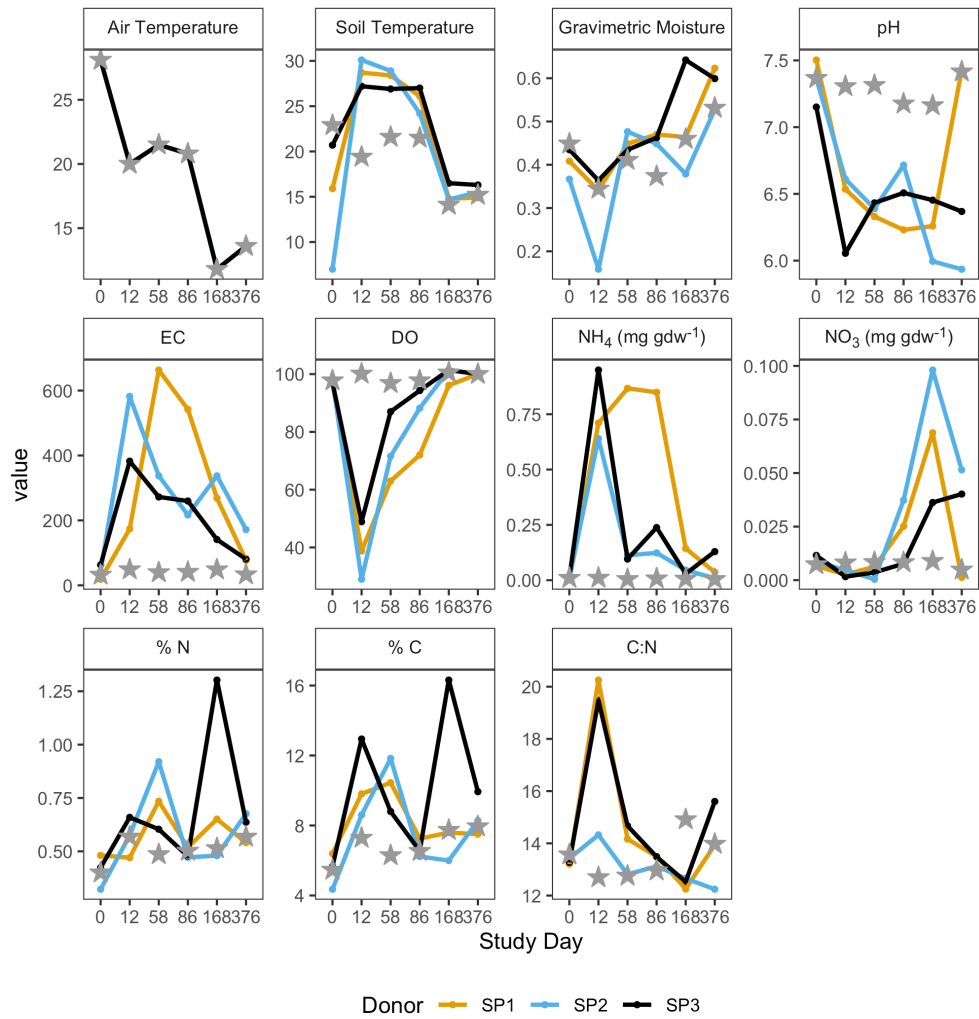
1831
1832

1833
1834

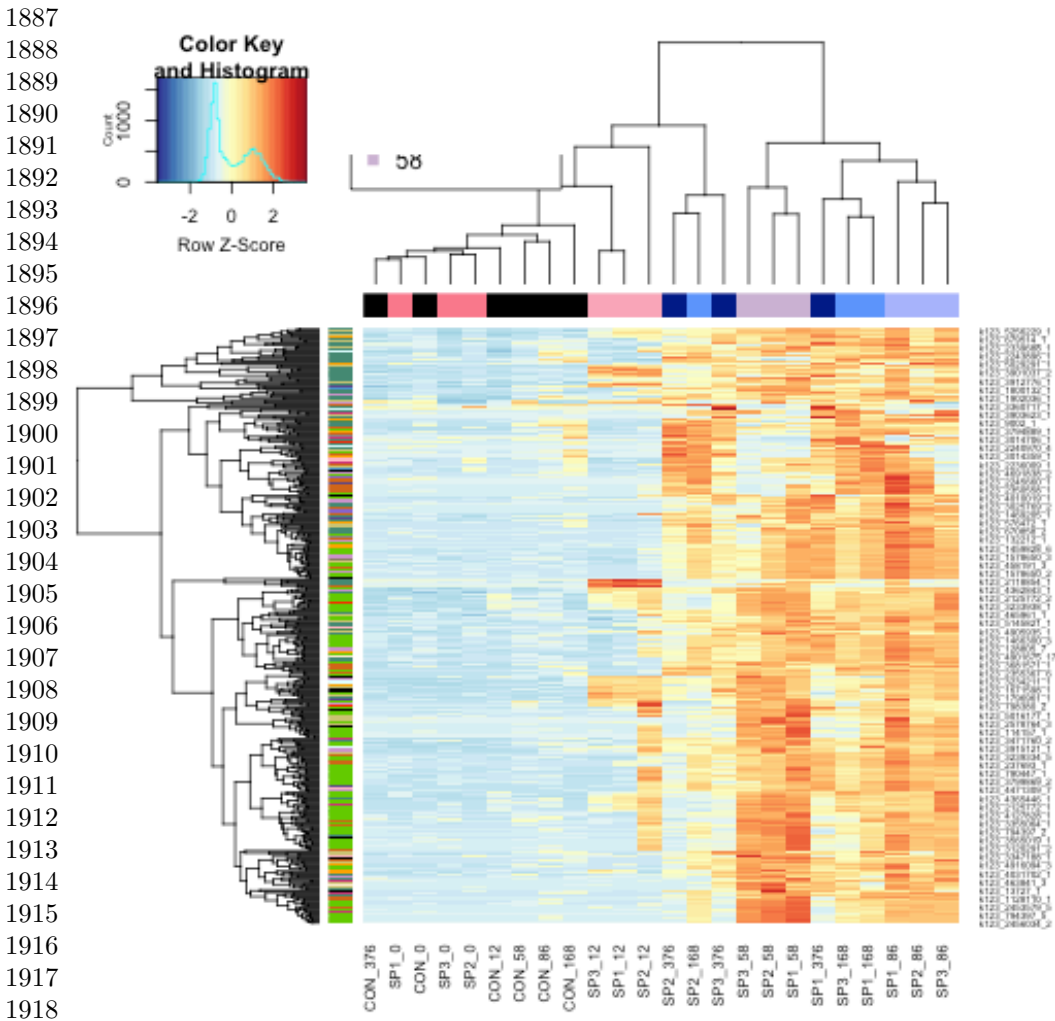
1835
1836

1837
1838

1839
1840



Supplementary Material 1: Figure S1. Soil physiochemical parameters in decomposition soils during the one-year study. Data is shown for each individual donor: SP1 (gold), SP2 (blue), and SP2 (black). Values for the full 16 cm core samples were estimated by summing values interface (0-1 cm) and core (0-16 cm) reported by Taylor et al, (2024) in 1:16 and 15:16 ratios, respectively. Controls reported here are means of three experimental controls that were unimpacted by decomposition and are represented by stars.

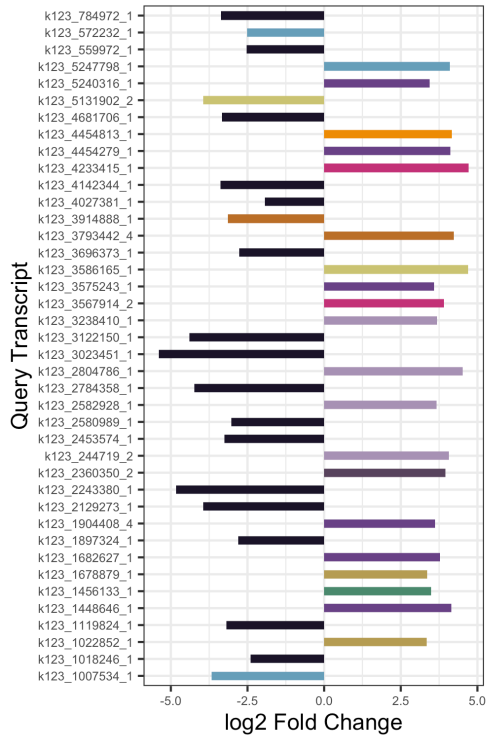


Supplementary Material 2: Figure S2. Hierarchical clustering heatmap showing the log counts per million (CPM) of the top 500 most variable genes across samples. Variable genes were determined by selecting genes with the highest variance in gene expression. Samples are clustered along the x-axis using Euclidean distances between samples and colored by study day.

Table S1. Permutational analysis of variance (PERMANOVA) results identifying significant environmental parameters which explain some of the variation in soil gene expression profiles. Environmental parameter data is from Taylor et al. (2024). Variables with $p < 0.05$ are indicated in bold.

Supplementary Material 3

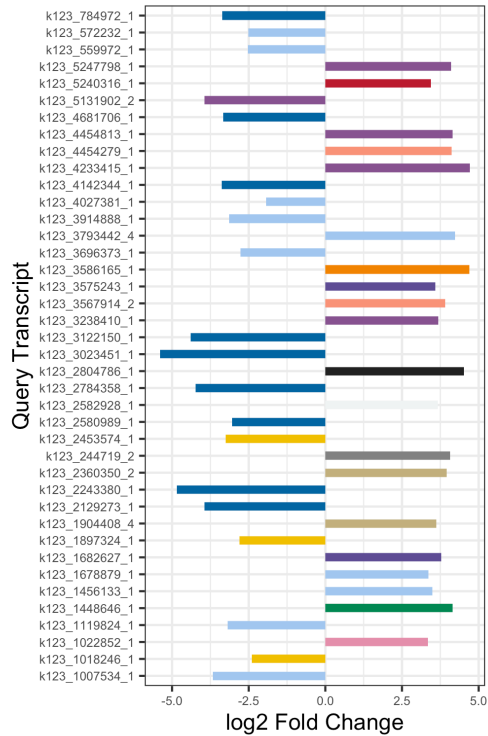
A



COG Category

- Cell motility
- Energy production and conversion
- Transcription
- Cell cycle control, cell division, chromosome partitioning
- Carbohydrate transport and metabolism
- Intracellular trafficking, secretion and vesicular transport
- Signal transduction mechanisms
- Translation, ribosomal structure and biogenesis
- Post-translational modification, protein turnover, and ch:
- Function Unknown
- unclassified

B



Taxonomy

- 1117|Cyanobacteria
- 1236|Gammaproteobacteria
- 135614|Xanthomonadales
- 2|Bacteria
- 200940|Thermodesulfobacteria
- 201174|Actinobacteria
- 203682|Planctomycetes
- 204432|Acidobacteriia
- 2157|Archaea
- 28211|Alphaproteobacteria
- 28221|Deltaproteobacteria
- 4751|Fungi
- 57723|Acidobacteria
- 976|Bacteroidetes

Supplementary Material 4: Figure S3. Top 40 up- and down-regulated genes in controls relative to decomposition soils across all study days, colored by COG functional category (A) and taxonomic annotation (B). Positive values denote higher expression in controls, while negative values are higher in decomposition soils.

1933
1934
1935
1936
1937
1938
1939
1940
1941
1942
1943
1944
1945
1946
1947
1948
1949
1950
1951
1952
1953
1954
1955
1956
1957
1958
1959
1960
1961
1962
1963
1964
1965
1966
1967
1968
1969
1970
1971
1972
1973
1974
1975
1976
1977
1978

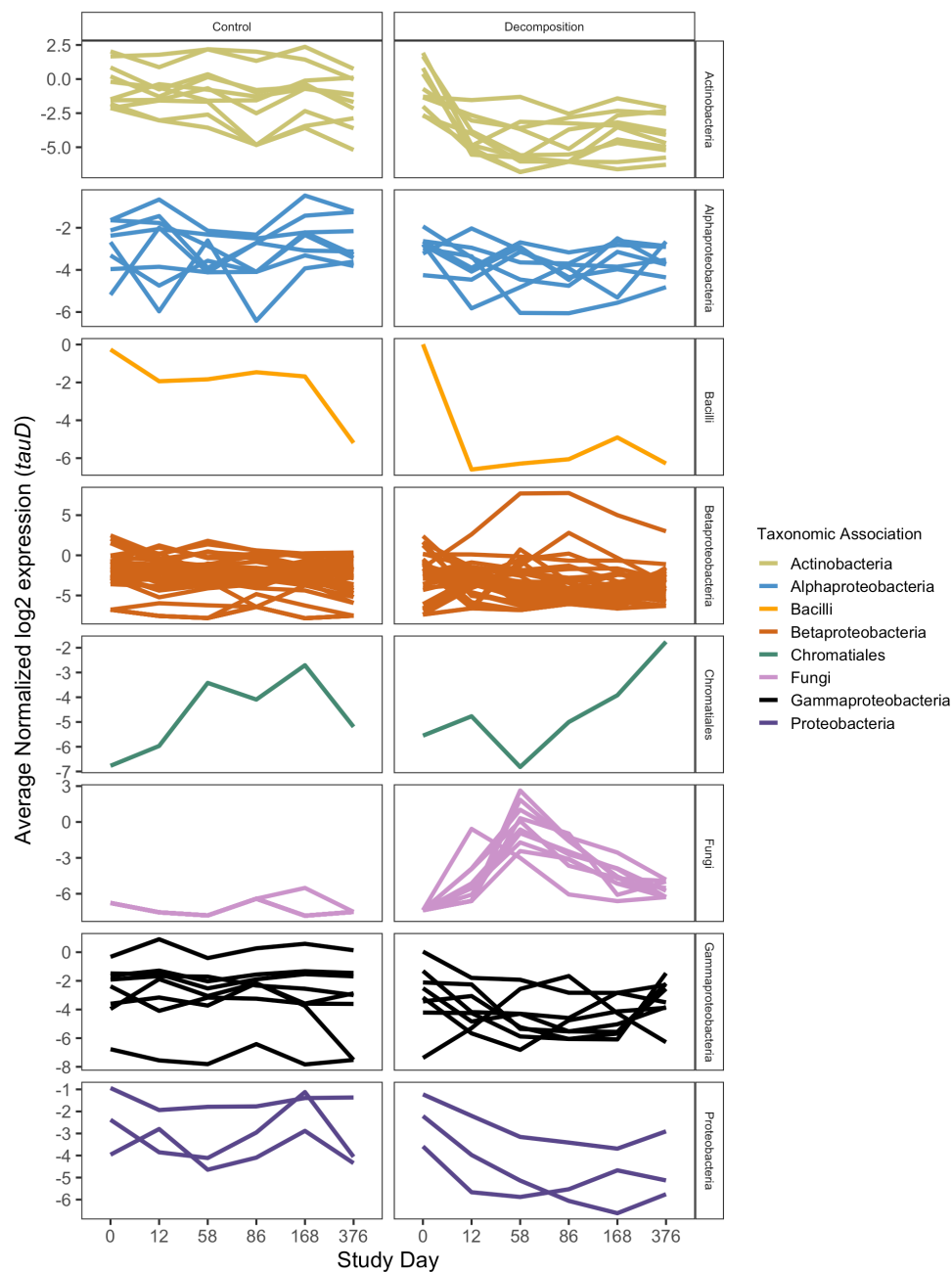
1979
1980
1981
1982
1983
1984
1985
1986
1987
1988
1989
1990
1991
1992
1993
1994
1995
1996
1997
1998
1999
2000
2001
2002
2003
2004
2005
2006
2007
2008
2009
2010
2011
2012
2013
2014
2015
2016
2017
2018
2019
2020
2021
2022
2023
2024

Table S2. Top 20 most up- and down-regulated gene queries, determined by log2 fold change and adjusted p-values, in control relative to decomposition soils. Positive log2 fold change values represent genes whose expression was higher in control soils, while negative log2 fold change values were higher in decomposition soils. Taxonomic annotation, COG categories, gene description, gene names, and EC were assigned via eggNOG-mapper.

Supplementary Material 5

Table S3. Top 10 most up- and down-regulated genes, determined by log2 fold change and adjusted p-values, for each sequential timepoint comparison. Positive log2 fold change values represent genes whose expression was higher in the later decomposition timepoint soils, while negative log2 fold change values are higher in earlier decomposition timepoint soils. Taxonomic annotation, COG categories, gene names, and EC were assigned via eggNOG-mapper. The comparison column distinguishes each timepoint comparison.

Supplementary Material 6



Supplementary Material 7: Figure S4. Mean normalized log₂ expression of *tauD* genes by taxonomic association (color) in control and decomposition soils at each study day. Each line represents one *tauD* gene query, while color denotes taxonomic association as determined by eggNOG-mapper.